J|A|C|S
COMMUNICATIONS

Published on Web 05/08/2007

Preferential End Functionalization of Au Nanorods through Electrostatic Interactions

P. Pramod, S. T. Shibu Joseph, and K. George Thomas*

Photosciences and Photonics, Regional Research Laboratory (CSIR), Trivandrum 695 019, India

Received March 5, 2007; E-mail: georgetk@md3.vsnl.net.in

Integration of nanoscale building blocks into higher-order assemblies and tuning their optoelectronic properties are of significant importance in the design of nanoscale devices.[1−6] Dimensionality of nanomaterials plays a crucial role in their assembly; for example, anisotropic one-dimensional (1D) nanomaterials can be more easily organized compared to isotropic spherical nanoparticles.[2−6] Among various ID nanomaterials, Au nanorods have gained much attention in recent years due to their wide range of applications as "interconnectors" in nanoscale devices,[3a] catalytic motors,[7] and photothermal therapy of tumor cells.[8] Several approaches have been reported for assembling Au nanorods which include (i) the design of bimetallic rods through electrochemical[3] and chemical methods,[5c] (ii) utilization of streptavidin−biotin interactions for end-to-end organization[4a−c] and decorating with nanoparticles,[4d] (iii) organization through electrostatic interactions,[5a,b] and (iv) longitudinal assembly through H-bonding/covalent methods.[6] Even though significant progress has been made in the organization of nanomaterials, site-specific functionalization still remains a major challenge. Herein we report a new methodology for the preferential end functionalization of Au nanorods with Au nanoparticles by exploiting the electrostatic attractive interactions (Scheme 1).

Ethylene glycol-protected Au nanoparticles having varying diameters (1.8−5.7 nm) were synthesized[9a] (Supporting Information), and their zeta potentials (ζ) were investigated. Interestingly, the ζ values varied linearly with particle size (+10 to +36 mV) due to the increase in their surface charge density (Figure 1A); however, the solvent polarity (CH_3CN/H_2O) has only little effect. In contrast, the ζ of Au nanorods varied from high positive values (Figure 1A; +39.8 ± 2 mV in deionized H_2O) to a high negative value (−39.6 ± 1 mV in 99% CH_3CN/H_2O) by varying the solvent polarity. The decrease in the ζ of Au nanorods to negative values with an increase in the composition of aprotic solvent may be due to the reorganization of the CTAB bilayer and their loss from the surface.[9b,c] The rationale behind the Au rod−particle electrostatic interaction is based on the fact that the nanorods possess high negative ζ values (−28.5 ± 1 mV) and Au nanoparticles have positive ζ values (e.g., 10 ± 0.5 mV for a 1.8-nm size particle) in a mixture (4:1) of CH_3CN and H_2O. In the present case, we have conveniently used this electrostatic attraction for the hierarchical integration of nanomaterials, and these aspects were investigated by UV−visible spectroscopic studies and HRTEM analysis.

Gold nanorods possess two plasmon bands (e.g. trace a, Figure 1B); a shorter wavelength band at 520 nm originating from the transverse plasmon oscillation and a longer wavelength band at 760 nm originating from the longitudinal plasmon oscillation. Microliter quantities of 1.8-nm Au nanoparticles (plasmon band peaks at 520 nm) were added to Au nanorods in a mixture (4:1) of CH_3CN/H_2O, and spectral changes were monitored. Interestingly, a spontaneous bathochromic shift in the longitudinal plasmon band of Au nanorods was observed on addition of nanoparticles; however,

Scheme 1. Schematic Representation for the Site-Specific Functionalization of Au Nanorods

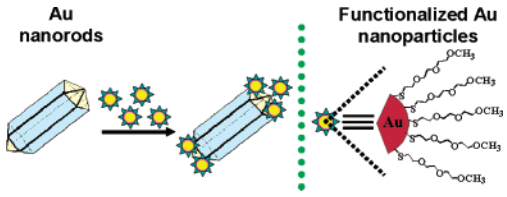

the position of the transverse plasmon band remained unaffected (Figure 1B). The enhanced intensity of the transverse band around 520 nm is due to the presence of excess nanoparticles in the solution. To better understand the interaction, absorption spectral changes were monitored by varying the nanoparticle diameter (1.8, 2.7, 4.5, and 5.7 nm) and the Au nanorod aspect ratio (2.2, 3.0, and 3.7). It is clear from the 3D plot presented in Figure 1C that the bathochromic shift in the longitudinal plasmon band ($\Delta\lambda$) is more pronounced for nanoparticles having smaller diameters, irrespective of the aspect ratio of Au nanorods. For example, a bathochromic shift of ~60 nm was observed on addition of 1.8-nm nanoparticles to Au nanorods (aspect ratio 3.7), whereas the shift is less pronounced for nanoparticles having diameters of 2.7 and 4.5 nm ($\Delta\lambda$ of 45 and 15 nm, respectively). Surprisingly no spectral shifts were observed on addition of 5.7-nm nanoparticles to Au nanorods (Figure 1D, vide infra).

The shift in the longitudinal plasmon absorption band can result either through an interplasmon coupling or a preferential binding

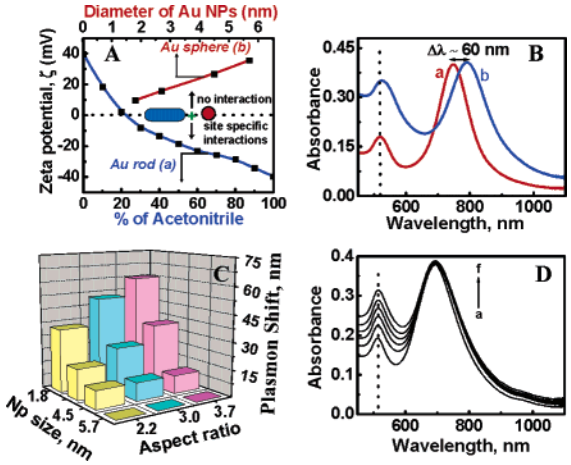

Figure 1. (A) Variation of ζ of (a) Au nanorods (aspect ratio of 3.7) at different compositions of CH_3CN/H_2O and (b) Au nanoparticles in a mixture (4:1) of CH_3CN/H_2O as a function of diameter. (B) Absorption spectra of Au nanorods (aspect ratio of 3.7) on addition of Au nanoparticles (diameter 1.8 nm) in a mixture (4:1) of CH_3CN/H_2O (a) 0 nM and (b) 10 nM. (C) Three-dimensional plot showing longitudinal plasmon shift of Au nanorods of different aspect ratios on addition of Au nanoparticles of varying diameters. (D) Absorption spectra of Au nanorods (aspect ratio of 3.0) on addition of 5.7-nm Au nanoparticles (a) 0 nM to (f) 30 nM.

10.1021/ja071536o CCC: $37.00

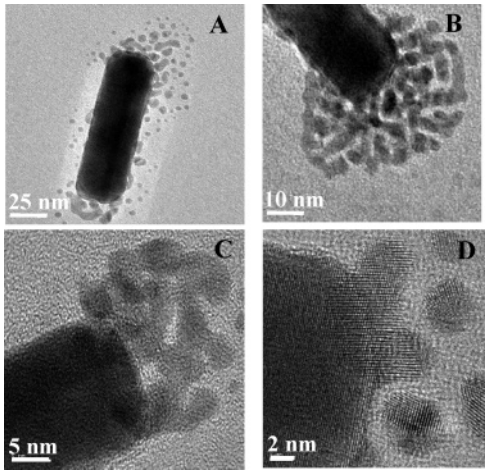

Figure 2. (A−D) HRTEM images of Au nanorods (aspect ratio of 3.7) recorded in the presence of Au nanoparticles (diameter 2.7 nm) from different locations of the grid.

of Au nanoparticles at the edges of Au nanorods. We have recently reported interplasmon coupling in Au nanorods which results in a gradual decrease in the longitudinal plasmon absorption along with concomitant formation of a new red-shifted band through a clear isosbestic point.[6] In the present case, a spontaneous red-shift in the longitudinal plasmon band was observed, and the mechanism involving the interplasmon coupling was ruled out. In an earlier report, Gluodenis and Foss have theoretically proposed a red-shift in the longitudinal plasmon band of Au nanorods when nanoparticles approach them in an end-to-end fashion.[10] In the present case, the bathochromic shift in the longitudinal plasmon band may be thus attributed to the selective binding of nanoparticles onto the edges of Au nanorods, leading to their preferential longitudinal growth. This was further confirmed using high-resolution transmission electron microscope (HRTEM) studies (Figure 2, A−D). HRTEM images clearly indicate the preferential close packing of Au nanoparticles on the edges of Au nanorods. This causes a change in the frequency of longitudinal plasmon oscillation, resulting in a bathochromic shift.

The obvious question is why do the nanoparticles preferentially bind onto the edges of Au nanorods? In a recent report, Pérez-Juste et al. have found that the electrical double-layer gradient is maximum at the edges of Au nanorods which accounts for their 1D growth.[5c,11] Also, the edges may be less protected with the surfactant compared to the lateral face. In the present case nanorods have negative ζ values (4:1 CH_3CN/H_2O), and the enhanced potential at their edges preferentially attracts the positively charged nanoparticles, leading to the selective growth of Au nanorods in the longitudinal direction. Further experiments were carried out in water wherein both nanorods and nanoparticles possess positive ζ values, and no spectral changes were observed, confirming the role of electrostatic attraction.

One of the interesting observations in the present case is the size dependency of nanoparticles on the relative shift in the longitudinal plasmon absorption band (Figure 1C, vide supra). In order to obtain quantitative information on the spectral shift, we have estimated the maximum number of nanoparticles that can be accommodated at the edge of nanorods as a function of their size (based on a close-packing model, the approximate numbers for 1.8-, 2.7-, 4.5-, and 5.7-nm nanoparticles are 350, 145, 75, and 30 respectively). The interparticle repulsion between the nanoparticles is much lower in the case of 1.8-nm nanoparticles ($+10 \pm 0.5$ mV), and nanorods can accommodate relatively more nanoparticles at the edges due to their smaller size, resulting in a larger plasmon shift. In contrast, the enhanced interparticle repulsion experienced by 5.7-nm nanoparticles (ζ of $+36 \pm 0.5$ mV) prevents them from binding onto the edges (HRTEM images in Supporting Information).

Similar spectral changes were observed with octylmercaptan-protected Au nanoparticles; however, the stability of the hybrid system was much lower compared to that of the ethylene glycol-protected Au nanoparticles.[12] The polar ethylene glycol moieties present on the surface of Au nanoparticles stabilize these hybrid nanostructures in polar solvent compared to the alkyl groups. In summary, we have demonstrated a novel methodology for the preferential functionalization of Au nanoparticles on the edges of Au nanorods through an electrostatic attraction. Moreover, these concepts can be utilized for connecting nanorods onto microelectrodes, alloying specific domains of nanorods and functionalizing chromophores on their edges. Site-specific functionalization methodology presented here may have potential application in the nanoscale fabrication of optoelectronic devices.

Acknowledgment. We thank the CSIR and the DST (SP/55/NM-75/2002), Government of India, for financial support. We thank Professor T. Pradeep, IIT Madras for HRTEM and Dr. Willi Paul, Sree Chitra Thirunal Institute of Medical Sciences and Technology, Trivandrum for ζ measurements. This is contribution RRLT-PPD-243 from RRL-T.

Supporting Information Available: Details on the synthesis of Au nanorods and nanoparticles and their interactions. This material is available free of charge via the Internet at http://pubs.acs.org.

References

(1) (a) Liz-Marzan, L. M. *Langmuir* **2006**, *22*, 32. (b) Burda, C.; Chen, X.; Narayanan, R.; El-Sayed, M. A. *Chem. Rev.* **2005**, *105*, 1025. (c) Murphy, C. J.; Sau, T. K.; Gole, A. M.; Orendorff, C. J.; Gao, J.; Gou, L.; Hunyadi, S. E.; Li, T. *J. Phys. Chem. B* **2005**, *109*, 13857. (d) Kelly, K. L.; Coronado, E.; Zhao, L. L.; Schatz, G. C. *J. Phys. Chem. B* **2003**, *107*, 668. (e) Shenhar, R.; Rotello, V. M. *Acc. Chem. Res.* **2003**, *36*, 549. (f) Thomas, K. G.; Kamat, P. V. *Acc. Chem. Res.* **2003**, *36*, 888.

(2) (a) Mokari, T.; Rothenberg, E.; Popov, I.; Costi, R.; Banin, U. *Science* **2004**, *304*, 1787. (b) Lin, S.; Li, M.; Dujardin, E.; Girard, C.; Mann, S. *Adv. Mater.* **2005**, *17*, 2553. (c) DeVries, G. A.; Brunnbauer, M.; Hu, Y.; Jackson, A. M.; Long, B.; Neltner, B. T.; Uzun, O.; Wunsch, B. H.; Stellacci, F. *Science* **2007**, *315*, 358.

(3) (a) Kovtyukhova, N. I.; Martin, B. R.; Mbindyo, J. K. N.; Smith, P. A.; Razavi, B.; Mayer, T. S.; Mallouk, T. E. *J. Phys. Chem. B* **2001**, *105*, 8762. (b) Martin, B. R.; Dermody, D. J.; Reiss, B. D.; Fang, M.; Lyon, L. A.; Natan, M. J.; Mallouk T. E. *Adv. Mater.* **1999**, *11*, 1021.

(4) (a) Caswell, K. K.; Wilson, J. N.; Bunz, U. H. F.; Murphy, C. J. *J. Am. Chem. Soc.* **2003**, *125*, 13914. (b) Salant, A.; Sadovsky, E. A.; Banin, U. *J. Am. Chem. Soc.* **2006**, *128*, 10006. (c) Zareie, M. H.; Xu, X.; Cortie, M. B. *Small* **2007**, *3*, 139. (d) Pierrat, S.; Zins, I.; Breivogel, A.; Sonnichsen, C. *Nano Lett.* **2007**, *7*, 259.

(5) (a) Gole, A.; Orendorff, C. J.; Murphy, C. J. *Langmuir* **2004**, *20*, 7117. (b) Correa-Duarte, M. A.; Perez-Juste, J.; Sanchez-Iglesias, A.; Giersig, M.; Liz-Marzan, L. M. *Angew. Chem., Int. Ed.* **2005**, *44*, 4375. (c) Grzelczak, M.; Perez-Juste, J.; Garcia de Abajo, F. J.; Liz-Marzan, L. M. *J. Phys. Chem. C* **2007**, *111*, 6183.

(6) (a) Thomas, K. G.; Barazzouk, S.; Ipe, B. I.; Joseph, S. T. S.; Kamat, P. V. *J. Phys. Chem. B* **2004**, *108*, 13066. (b) Sudeep, P. K.; Joseph, S. T. S.; Thomas, K. G. *J. Am. Chem. Soc.* **2005**, *127*, 6516. (c) Joseph, S. T. S.; Ipe, B. I.; Pramod, P.; Thomas, K. G. *J. Phys. Chem. B* **2006**, *110*, 150.

(7) Paxton, W. F.; Kistler, K. C.; Olmeda, C. C.; Sen, A.; St. Angelo, S. K.; Cao, Y.; Mallouk, T. E.; Lammert, P. E.; Crespi, V. H. *J. Am. Chem. Soc.* **2004**, *126*, 13424.

(8) Huang, X.; El-Sayed, I. H.; Qian, W.; El-Sayed, M. A. *J. Am. Chem. Soc.* **2006**, *128*, 2115.

(9) (a) Foos, E. E.; Snow, A. W.; Twigg, M. E.; Ancona, M. G. *Chem. Mater.* **2002**, *14*, 2401. (b) Takahashi, H.; Niidome, Y.; Niidome, T.; Kaneko, K.; Kawasaki, H.; Yamada, S. *Langmuir* **2006**, *22*, 2. (c) Gole, A.; Murphy, C. J. *Chem. Mater.* **2005**, *17*, 1325.

(10) Gluodenis, M.; Foss, C. A. *J. Phys. Chem. B* **2002**, *106*, 9484.

(11) Pérez-Juste, J.; Liz-Marzán, L. M.; Carnie, S.; Chan, D. Y. C.; Mulvaney, P. *Adv. Funct. Mater.* **2004**, *14*, 571.

(12) Assembly based on octylmercaptan-capped Au particles precipitate in 15 min, whereas the assembly based on Au nanoparticles is stable for more than 3 h (slow precipitation was observed at longer periods).

JA071536O